Effects of systemic inhibitors of Acid-Sensing Ion Channels 1 (ASIC1) against acute and chronic mechanical allodynia in a rodent model of migraine

Running title: ASIC1 channel inhibitors against acute and chronic migraine

Clément Verkest[1,2,3], Emilie Piquet[3,4], Sylvie Diochot[1,2,3], Mélodie Dauvois[1], Michel Lanteri-Minet[3,4,5], Eric Lingueglia[1,2,3, *, #], Anne Baron[1,2,3, *, #]

[1]: Université Côte d'Azur, CNRS, Institut de Pharmacologie Moléculaire et Cellulaire, France.

[2]: LabEx Ion Channel Science and Therapeutics, Valbonne, France.

[3]: FHU InovPain, Université Côte d'Azur, Nice, France.

[4]: CHU Nice, Hopital Cimiez, Département d'évaluation et de traitement de la douleur, Nice, France.

[5]: Inserm/UdA, U1107, Neuro-Dol, Trigeminal Pain and Migraine, Université d'Auvergne, France.

* E.L. and A.B. contributed equally to this work.

[#] Corresponding authors.

Author contributions

CV, EP, MLM, EL and AB designed research; CV, EP, SD, MD, AB performed research and SD, CV, MLM, EL and AB wrote the paper.

Main body word count (Results +Discussion): 3477

This article has been accepted for publication and undergone full peer review but has not been through the copyediting, typesetting, pagination and proofreading process which may lead to differences between this version and the Version of Record. Please cite this article as doi: 10.1111/bph.14462

Acknowledgments

We thank R. Dallel for initial help with the ISDN-induced model in rats and discussion, D. Servent for providing synthetic mambalgin-1, E. Deval, P. Inquimbert, J. Noël, M. Salinas, M. Chafai, S. Marra and T. Besson for helpful discussions, M. Lazdunski for his support, V. Friend for expert technical assistance, and V. Berthieux for secretarial assistance. This work was supported by CNRS, Inserm, the Fondation pour la Recherche Medicale (DEQ20110421309) and the Agence Nationale de la Recherche (ANR-13-BSV4-0009, ANR-17-CE18-0019, and ANR-11-LABX-0015-01).

Conflict of interest statement

The authors declare no conflict of interest.

ATP:
http://www.guidetopharmacology.org/GRAC/LigandDisplayForward?ligandId=1713
Nitric oxide :
http://www.guidetopharmacology.org/GRAC/LigandDisplayForward?ligandId=2509
Nitroglycerin:
http://www.guidetopharmacology.org/GRAC/LigandDisplayForward?ligandId=7053
Isosorbide dinitrate:
http://www.guidetopharmacology.org/GRAC/LigandDisplayForward?ligandId=7052
CGRP:
http://www.guidetopharmacology.org/GRAC/LigandDisplayForward?ligandId=695
Sumatriptan:
http://www.guidetopharmacology.org/GRAC/LigandDisplayForward?ligandId=54
Propranolol:
http://www.guidetopharmacology.org/GRAC/LigandDisplayForward?ligandId=564
Topiramate:
http://www.guidetopharmacology.org/GRAC/LigandDisplayForward?ligandId=6849
ASICs:
http://www.guidetopharmacology.org/GRAC/FamilyDisplayForward?familyId=118
Mambalgins:
http://www.guidetopharmacology.org/GRAC/FamilyDisplayForward?familyId=118
Amiloride:
http://www.guidetopharmacology.org/GRAC/LigandDisplayForward?ligandId=2421
5-HT1B/1D receptor:
http://www.guidetopharmacology.org/GRAC/ObjectDisplayForward?objectId=2
Epithelial sodium channel:
http://www.guidetopharmacology.org/GRAC/FamilyDisplayForward?familyId=122
TRPV1:
http://www.guidetopharmacology.org/GRAC/ObjectDisplayForward?objectId=507

Abstract

Background and purpose

Acid-Sensing Ion Channels (ASICs) are neuronal proton sensors emerging as potential therapeutic targets in pain of the orofacial region. Amiloride, a non-specific ASIC blocker, has been shown to exert beneficial effects in animal models of migraine and in patients. We explored the involvement of the ASIC1-subtype in cutaneous allodynia, a hallmark of migraine affecting cephalic and extra-cephalic regions in about 70% of migrainers.

Experimental approach

We investigated the effects on cephalic and extra-cephalic mechanical sensitivity of systemic injections of amiloride and mambalgin-1, a specific inhibitor of ASIC1a- and ASIC1b-containing channels, in a rodent model of acute and chronic migraine induced by intraperitoneal injections of isosorbide dinitrate.

Key results

Intravenous injection of these inhibitors reversed cephalic and extra-cephalic acute cutaneous mechanical allodynia in rats, a single injection inducing a delay in the subsequent establishment of chronic allodynia. Mambalgin-1 or amiloride also reversed established chronic allodynia. The anti-allodynic effect of mambalgin-1 was not altered in ASIC1a-knock-out mice, showing no contribution of the ASIC1a subtype in the effect.. Mambalgin-1 anti-allodynic effects are comparable to the ones of the anti-migraine drug sumatriptan and of the preventive drug topiramate on acute and chronic allodynia, respectively. A single daily injection of mambalgin-1 also had a significant preventive effect on allodynia chronification.

Conclusions and Implications

These pharmacological data support the involvement of peripheral ASIC1-containing channels in migraine cutaneous allodynia as well as in its chronification. They highlight the therapeutic potential of ASIC1 inhibitors in migraine for both acute and prophylactic treatment.

Abbreviations

ASIC: Acid-sensing Ion channel

Mamb-1: mambalgin-1

CSD: cortical spreading depression

TG: trigeminal

NO: nitric oxide

ISDN: isosorbide dinitrate

TNC: trigeminal nucleus caudalis

CGRP: calcitonin gene-related peptide

i.pl.: intraplantar

KO: knock-out

Keywords:

ASIC, mambalgin, migraine, allodynia, amiloride

Introduction

Migraine is a major contributor to public ill health (Vos *et al.*, 2016) with still poorly understood pathogenetic mechanisms (Goadsby *et al.*, 2017) possibly including extracellular acidification. Cortical spreading depression (CSD), considered to be the neurophysiological correlate of migraine aura, could activate and sensitize trigeminal (TG) meningeal nociceptors (Karatas *et al.*, 2013) through local release of extracellular compounds (K^+, ATP, nitric oxide), dural sterile inflammation and ischemia associated with extracellular acidification also involving mast cells degranulation (Rozniecki *et al.*, 1999; Levy, 2009). Subsequent sensitization of central pathways would cause cephalic and extra-cephalic cutaneous allodynia (Edelmayer *et al.*, 2009; Burstein *et al.*, 2010; Boyer *et al.*, 2014) reported by 70% of migrainers during migraine attacks (Lipton *et al.*, 2008). Per year, approximately 2.5% of episodic migrainers become chronic migrainers, with at least 15 days of headache per month (Bigal *et al.*, 2008; Lipton *et al.*, 2015), showing acute cutaneous allodynia during attacks but also interictal allodynia between them (Nahman-Averbuch *et al.*, 2018). Cutaneous allodynia is now considered as a marker and a risk factor for chronic migraine (Louter *et al.*, 2013), chronic migraine onset being increased by 30% among episodic migrainers, and chronic migraine persistence being increased by 15% in chronic migrainers (Scher *et al.*, 2017).

Preclinical migraine models in rodents are based on human observations. Nitric oxide (NO) donors such as nitroglycerin (NTG) (Ashina *et al.*, 2013) and nitrate-based drugs with slower pharmacokinetics like isosorbide dinitrate (ISDN) used in the treatment of cardiovascular disease (Iversen *et al.*, 1992; Olesen & Ashina, 2015; Hansen & Olesen, 2017), trigger a delayed-migraine attack associated with cutaneous facial and extra-facial allodynia (Thomsen *et al.*, 1996). In rodents, NO donors evoke elevated CGRP blood levels, meningeal inflammation, photo- and phonophobia, sensitization of central neurons of the trigeminal nucleus caudalis (TNC), cephalic and extra-cephalic allodynia, as well as

spontaneous facial pain. The efficiency of clinically relevant treatments like sumatriptan, CGRP antagonists and antibodies, anti-inflammatory drugs, or prophylactic drugs like propranolol and topiramate further support the relevance of these animal models of migraine (Bates *et al.*, 2010; Jansen-Olesen *et al.*, 2013; Pradhan *et al.*, 2014; Farkas *et al.*, 2016; Goadsby *et al.*, 2017; Harris *et al.*, 2017; Schytz *et al.*, 2017). Effects of systemic ISDN injections were recently described in rats, with a facilitation of C-fiber-evoked responses in 50% of second-order central neurons (Flores Ramos *et al.*, 2017; Dallel *et al.*, 2018), leading to cutaneous pain sensitization.

Acid-Sensing Ion Channels (ASICs) are voltage-insensitive cation channels activated by extracellular acidosis (ASIC1-3) (Waldmann *et al.*, 1997) and lipids (ASIC3) (Marra *et al.*, 2016). They are widely expressed throughout the peripheral and central nervous system where they have been implicated in various pathophysiological processes including pain (Deval & Lingueglia, 2015). Most subunits are expressed in TG neurons, where ASIC1- and ASIC3-containing channels can contribute to activation of meningeal afferents (Yan *et al.*, 2011; Yan *et al.*, 2013) and in migraine pathophysiology (Dussor, 2015). ASIC1a and 2a are expressed by second-order neurons of the TNC (Cho *et al.*, 2015), and brain ASIC1a-containing channels have been implicated in CSD (Holland *et al.*, 2012).

Peptide toxins from animal venoms specifically targeting different ASIC subtypes have been instrumental to reveal their roles in pain (Mazzuca *et al.*, 2007; Deval *et al.*, 2008; Bohlen *et al.*, 2011; Baron *et al.*, 2013), including mambalgins that exert potent analgesic effects against acute, inflammatory and neuropathic pain through specific inhibition of ASIC1a- and/or ASIC1b-containing channels (Diochot *et al.*, 2012; Diochot *et al.*, 2016). Using mambalgin-1 (Mamb-1) in combination with amiloride, a non-specific ASICs blocker, we explored here the involvement of ASIC1-containing channels in mechanical cephalic and extra-cephalic cutaneous allodynia in the ISDN-induced model of migraine in rodents.

Methods

Animals

Experiments were performed on male Sprague Dawley rats (Janvier Labs) weighting 250 to 400g (mean weight: 306 ± 12g, 6 to 9 weeks old), and on male C57BL/6J wild-type (Charles River Laboratories) and ASIC1a-knock-out mice (Wemmie *et al.*, 2002) of 7-13 week-old weighting 20-25g. Animals were housed in a 12 hours light-dark cycle with food and water available ad libitum. Animal studies are reported in compliance with the ARRIVE

guidelines (Kilkenny *et al.*, 2010; McGrath & Lilley, 2015). Animal procedures were approved by the Institutional Local Ethical Committee and authorized the French Ministry of Research according to the European Union regulations and the Directive 2010/63/EU (Agreements C061525 and 01550.03). Animals were sacrificed at experimental end points by CO_2 euthanasia.

Drugs and in vivo injections

Synthetic Mamb-1, showing the same pharmacological activity than native peptide, was purchased from Synprosis/Provepep (Fuveau, France), Smartox (Saint Martin d'Hères, France), or obtained from Commissariat à l'Energie Atomique, iBiTecS, Service d'Ingénierie Moléculaire des Protéines (Gif sur Yvette, France) (Mourier *et al.*, 2016). The biological activity of all synthetic Mamb-1 batches was validated on heterologously expressed recombinant ASIC channels.

Mamb-1 was dissolved in vehicle solution containing NaCl 0.9% and bovine serum albumin 0.05% to prevent non specific toxin adsorption. For intravenous (*i.v.)* injections in rats, Mamb-1 (11.3 nmol/kg, i.e., 200 µl of 16.5 µM for a 300g rat), amiloride hydrochloride hydrate (10 mg/kg, i.e., 200 µl of 56 mM for a 300g rat, Sigma Aldrich), topiramate (30 mg/kg, i.e., 500 µl of 18mg/ml for a 300g rat, Selleckchem), all dissolved in vehicle solution, or sumatriptan succinate (10 mg/kg i.e., 250 µl of injectable 12 mg/ml solution for a 300g rat, Imiject®, GlaxoSmithKline) were injected in the caudal vein of conscious rats (restrained in a cylinder) with a 30G needle. For intraplantar subcutaneous (*i.pl.)* injections, Mamb-1 (6.7 nmol/kg, i.e., 50 µl of 41 µM for a 300g rat) was injected in the left hindpaw of conscious rats with a 26G needle. For mice, Mamb-1 (13.6 nmol/kg, i.e., 200 µl of 1.7 µM for a 25g mouse) dissolved in vehicle solution was *i.v.* injected in the caudal vein of conscious mice (restrained in a cylinder) with a 30G needle. The effects seen in our study with amiloride, sumatriptan and topiramate are consistent with the known pharmacokinetics of these drugs administered via the *i.v.* route in rodents.

Thermal and mechanical sensitivity measurements

Thermal sensitivity was assessed using the Hargreaves plantar test (Ugo Basile, Italy). Unrestrained rats were placed in individual plastic boxes on a glass floor. The withdrawal latency (s) of the rat hindpaw exposed to an infrared source (intensity of 190 ±1 mW/cm²) was measured in triplicate with at least 1min between two stimulations, and the mean latency was calculated. A cut-off period of 20s was used to avoid potential tissue damage. Rats were

trained 2 days before experiments. To test the effect of Mamb-1, thermal sensitivity was measured every 15 minutes before (basal value) and during two hours after Mamb-1 or vehicle injection.

The face mechanical sensitivity was measured using calibrated von Frey filaments (Bioseb, France). Unrestrained rats placed in individual plastic boxes on top of a wire surface boxes were trained over one week to stimulation on the periorbital area, following a progressive protocol, starting with non-noxious filaments during the first 3 days of training. The face withdrawal force threshold (g) was determined by the filament evoking at least 3 responses over five trials, starting with lower force filaments. To test the effect of ISDN, the face mechanical sensitivity was measured every 15 minutes before (basal value) and during three hours after intraperitoneal (*i.p.*) injection. To test the effect of Mamb-1 and other compounds, face mechanical sensitivity was measured every 15 minutes before (basal value) and during two hours after compound or vehicle injection.

The hindpaw mechanical sensitivity was evaluated with a dynamic plantar aesthesiometer (Ugo Basile, Italy). Unrestrained rats were placed in 6 individual plastic boxes on top of a wire surface. The rat hindpaw was submitted to a force ramp up to 30 g during 20 s, the paw withdrawal force threshold (g) was measured in triplicates, and the mean force was calculated. During five days, rats were habituated to repeated (every 15 min) measurements of face and hindpaw mechanical sensitivities, and basal values were determined 2 days before experiments. To test the effect of ISDN, the hindpaw mechanical sensitivity was measured every 15 minutes before (basal value) and during three hours after intraperitoneal (*i.p.*) injection. To test the effect of Mamb-1 and other drugs, the hindpaw mechanical sensitivity was measured every 15 minutes before (basal value) and during two hours after injection. For mice, the same procedure was used to measure the hindpaw mechanical sensitivity, except that a force ramp up to 7.5 g during 10 s was applied every 30 minutes, and that twelve mice could be tested simultaneously.

Pain and migraine rodent models

Local inflammation was induced by *i.pl.* injection in a rat left hindpaw of 100 µl of 2% carrageenan (Sigma-Aldrich) with a 25G needle. Thermal and mechanical sensitivity were measured before (basal values) and 3 hours after the carrageenan injection to measure thermal hyperalgesia and mechanical allodynia induced by inflammation (control values). Effects of drugs were followed by measurements every 15 min during 2 hours after their injection.

The rat model of NO-induced migraine was induced by intraperitoneal (*i.p.*) injection of ISDN (Risordan®, Sanofi) at 10mg/kg, a long-lasting NO donor, and was cited as ISDN-induced model in the text. The cephalic and hindpaw extra-cephalic mechanical sensitivities were measured simultaneously on the same rat. The acute mechanical allodynia induced by a single ISDN injection was followed for 3 hours after injection. Chronic mechanical allodynia was induced by a single daily injection of ISDN during 4 days. Cephalic and extra-cephalic mechanical sensitivity were measured each day before the ISDN *i.p.* injection. Drugs were tested on chronic mechanical allodynia on the 5^{th} day and effects were followed every 15 min during 2 hours after injection. This model has been transposed to mice according to the same protocol, except that only the hindpaw extra-cephalic mechanical sensitivity was measured.

Control (or vehicle treated) and test animals were randomized within experimental sessions. Drug and peptide injections were not performed blindly in these experiments (implemented since) and data collection, analysis and statistics were performed and validated by two independent experimenters.

Data and statistical analysis

For behavioral experiments, kinetics of effects were shown, displaying mean ± SEM in function of time was shown, along with cumulative effect over 2 hours after injection of drugs, or over 3 hours after ISDN injection, calculated as Area Under the Curve (AUC, g x min for mechanical sensitivity, or s x min for thermal sensitivity) subtracted from the control value for each animal and expressed as mean ± SEM with individual data points shown. Total effect (AUC) = $\sum$ dYxdT, with dY the relative variation Ymax-Ycontrol of the measured parameter (withdrawal force or latency), and dT the time interval between two successive measurements (usually 15 min).

The power calculation was performed with an alpha value of 0.05 and a power of 0.8 with G*Power software, to calculate the minimum sample size per group needed depending on the expected variability of measurements (which differs between behavioral tests) and the type of statistical test to be used. For example, for rat experiments, the minimal calculated sample size was 8 with effect sizes between 1.6 and 1.1. As most of our behavioral experiments and pharmacological treatments were not previously tested, and to anticipate the possible occurrence of non-respondent animals to pre-required treatments by carrageenan or ISDN, we set our usual minimal experimental sample size to 9. This “n” value refers to independent values and not technical replicates (replicates were used to calculate a mean

individual value). Control (or vehicle treated) animals and test animals were randomized within experimental days. Data are presented as mean values ± standard error of the mean (SEM). Data analysis and statistics were performed with Microcal Origin 6.0 and GraphPad Prism 4 softwares by two independent experimenters. The normality of data distribution was tested by KS normality test, D'Agostino & Pearson omnibus normality test and Shapiro-Wilk normality test, and parametric or non parametric tests were chosen for normal or non normal data distribution, respectively. Non parametric tests were used when the number of animals per experimental group was less than 10, because the results of normality tests were not fully reliable in these conditions. The statistical difference between two different experimental groups was analyzed by the parametric unpaired Student's *t*-test or by the non parametric Mann-Whitney test. The statistical difference between more than two different experimental groups was assessed by the parametric one-way analysis of variance (Anova) followed by a Tukey post-test, or by the non parametric Kruskall Wallis test followed by a Dunns post-test. For data within the same experimental group, a parametric paired Student's *t*-test or a non parametric Wilcoxon matched pair test were used. The level of probability $p<0.05$ denotes a statistically significant differences between groups, and post hoc tests were only run when $p<0.05$.

Nomenclature of Targets and Ligands

Key protein targets and ligands in this article are hyperlinked to corresponding entries in http://www.guidetopharmacology.org, the common portal for data from the IUPHAR/BPS Guide to PHARMACOLOGY (Harding *et al.*, 2018), and are permanently archived in the Concise Guide to PHARMACOLOGY 2017/18 (Alexander *et al.*, 2017).

Results

Anti-allodynic effects of *i.v.* mambalgin-1 against inflammatory pain in rats

Mambalgins exert analgesic effects in mice upon different routes of administration (*i.pl., i.v., i.t.*) and against different types of pain, including inflammatory pain (Diochot *et al.*, 2012; Diochot *et al.*, 2016). However, their effects in rats were never tested. Before using the ISDN-induced model of migraine for simultaneous measurements of cephalic and extra-cephalic mechanical sensitivity, we first determined the effect of Mamb-1 in inflammatory pain in rats by testing a single dose extrapolated from the maximal effective concentration previously determined in mice from an *in vivo* dose-response curve (Diochot *et al.*, 2016).

Three hours after *i.pl.* injection of 2% carrageenan in the hindpaw, mechanical allodynia was observed, with a decrease in withdrawal threshold force from 18.4 ± 0.5 down to 9.2 ± 0.2g (Fig. 1A), as well as thermal hyperalgesia, with a decrease in withdrawal latency from 9.0 ± 0.3 down to 4.3 ± 0.2s (Fig. 1B). Intravenous injection of Mamb-1 (11.3 nmol/kg) induced a complete and sustained reversal of the inflammatory-induced mechanical allodynia (Fig 1A, 19.1 ± 0.8g after 45 minutes), as well as a complete reversion of the inflammatory-induced thermal hyperalgesia (Fig. 1B, 8.7 ± 0.5s, after 45 minutes). Local *i.pl.* injection of Mamb-1 in the rat inflamed hindpaw (6.7 nmol/kg) also resulted in a complete and sustained reversal of the inflammatory-induced mechanical allodynia (Fig. 1C) and thermal hyperalgesia (Fig. 1D). The kinetics and total effects of Mamb-1 were comparable between *i.v.* and *i.pl.* injections (Fig. 1C-F). On the other hand, *i.pl.* and *i.v.* injections of Mamb-1 had no effect on hindpaw mechanical threshold in naive rats (Suppl. Fig. 1).

These data indicate that *i.v.* or *i.pl.* Mamb-1 exert anti-allodynic effects on inflammatory pain in rats, comparable to the effects we already described in mice that were mainly peripheral and caused by the inhibition of ASIC1b-containing channels (Diochot *et al.*, 2016).

Effect of *i.v.* mambalgin-1 and amiloride on acute cutaneous mechanical allodynia in the ISDN-induced model of migraine

The ISDN-induced chronic migraine model was developed recently in rats (Flores Ramos *et al.*, 2017; Dallel *et al.*, 2018), related to the chronic NTG-induced model first developed in mice (Pradhan *et al.*, 2014). One *i.p.* injection of ISDN (10 mg/kg) induces mechanical allodynia mimicking what is occurring during migraine attack, with a decrease in cephalic and extra-cephalic mechanical sensitivity. The facial and hindpaw withdrawal force thresholds reached their minimal values after 1.5 hours (3.3 ± 0.4 from a basal control value of 7.5 ± 0.3g; and 12.2 ± 0.4 from a basal control value of 17.8 ± 0.2g, respectively) that were maintained for at least 3 hours, whereas *i.p.* injections of saline were without effect (Suppl. Fig. 2A, B, black symbols, left panels). Twenty four hours later, an allodynia was still present, and one ISDN injection per day during four days resulted in the progressive development of a chronic basal mechanical allodynia (2.4 ± 0.3g on the face, and 10.1 ± 0.3g on the paw; Suppl. Fig. 2C, D), which was correlated with a progressive decrease in the ISDN-induced cephalic and extra-cephalic total effect on acute cutaneous allodynia, the last injection inducing no more significant effect (Suppl. Fig. 2A, B, right panels). The chronic

basal mechanical allodynia persisted several days after the last ISDN injection, and a nearly total reversion was observed 15 days after the end of ISDN treatment (Suppl. Fig. 2C, D).

The effect of *i.v.* Mamb-1 on the acute mechanical allodynia induced by the first ISDN injection was tested. When Mamb-1 was injected after the full development of acute allodynia (*i.e.*, 105 min after ISDN *i.p.* injection), it induced a full reversal of facial mechanical allodynia (Fig. 2A), the withdrawal force increasing from the allodynic value of 3.3 ± 0.5 up to 7.6 ± 0.4g one hour after the *i.v.* injection, which is not significantly different from the baseline (8.0 ± 0.3g). On the same animals, Mamb-1 only induced a partial reversal of the hindpaw mechanical allodynia, the withdrawal force increasing from the allodynic value of 11.2 ± 0.5 up to 14.0 ± 1.3g one hour after the *i.v.* injection (Fig. 2B). These effects were sustained for at least 2 hours. The anti-allodynic effect of *i.v.* Mamb-1, which significantly reduced the total effects of the first injection of ISDN on cutaneous allodynia, induced a one-day shift in the development of chronic allodynia induced by subsequent daily *i.p.* injections of ISDN in both cephalic and extra-cephalic territories, without any change in the maximal basal allodynia measured on the last day (Fig. 2C, D). This supports, as suggested in humans, a causality link between occurrence of attack-like mechanical allodynia and the development of chronic allodynia.

The effect of *i.v.* Mamb-1 on ISDN-induced acute mechanical allodynia was compared with the one of amiloride, a well-known non-selective inhibitor of ASICs, and also with the one of acute migraine therapy sumatriptan, a 5-HT1B/1D receptor agonist. Amiloride or sumatriptan succinate, both *i.v.* injected in the same conditions as Mamb-1, also exerted an anti-allodynic effect. Amiloride induced a full reversion of face mechanical allodynia (Fig. 3A) and a partial but significant reversion of hindpaw allodynia (Fig. 3B), similar to the sustained Mamb-1 effects. As expected from its therapeutical effect, and as previously described in mice models of migraine (Bates *et al.*, 2010; Pradhan *et al.*, 2014), sumatriptan also showed sustained anti-allodynic properties, with a partial reversion of both facial (Fig. 3A) and hindpaw (Fig. 3B) allodynia.

All together, these data show that systemic *i.v.* Mamb-1 and amiloride efficiently reverse the ISDN-induced cephalic, and to a lesser extent extra-cephalic, mechanical acute cutaneous allodynia, with an even higher potency than sumatriptan.

Effects of *i.v.* mambalgin-1 and amiloride on the maximal chronic cutaneous mechanical allodynia in the ISDN-induced model of migraine

When Mamb-1 was injected one day after the last ISDN injection (*i.e.*, on the fifth day), it fully reversed the maximal chronic facial mechanical allodynia (Fig. 4A), increasing the facial withdrawal force from 3.0 ± 0.4 up to 9.6 ± 2.1g after one hour, a value similar to baseline (8.6 ± 0.9g). Mamb-1 also partially reversed the maximal chronic hindpaw mechanical allodynia (Fig. 4B), increasing the paw withdrawal force from 9.8 ± 0.2 up to 15.0 ± 1.1g after one hour, which is significantly different from vehicle as well as from baseline (18.0 ± 0.2g). Amiloride also showed similar anti-allodynic effects (Fig. 4A, B). Both compounds were as potent as topiramate, a clinically used preventive drug against migraine, whereas sumatriptan used in acute migraine therapy was ineffective (Fig. 4C-F), as previously described (Pradhan *et al.*, 2014). Local *i.pl.* injection of Mamb-1, which was able to reverse inflammatory-induced mechanical paw allodynia (Fig 1C), was without effect on ISDN-induced chronic paw mechanical allodynia (Suppl Fig. 3) showing that the local inhibition of ASICs in sensory neurons of the paw was not involved in the anti-allodynic effet of Mamb-1 on the paw ISDN-induced allodynia, contrary to the effects on inflammatory pain. Furthermore, the absence of effect of *i.pl.* injection of Mamb-1 on chronic facial ISDN-induced allodynia (Suppl Fig. 3), contrary to what is observed after *i.v.* injection, confirmed that the effect of the peptide upon *i.pl.* injection remains local without important systemic diffusion towards blood.

These data show that systemic *i.v.* Mamb-1 and amiloride efficiently reverse the maximal chronic cephalic and extra-cephalic chronic cutaneous mechanical allodynia with a potency similar to topiramate.

Preventive effect of *i.v.* mambalgin-1 treatment on the development of chronic cutaneous mechanical allodynia in the ISDN-induced migraine model

Mamb-1 was able to reverse the maximal chronic cutaneous allodynia induced by four days of ISDN injections. We tested next the effects of one daily *i.v.* injection of Mamb-1 for four days, between ISDN-induced attacks, and their consequences on the development of chronic allodynia.

In good agreement with the data showing no effect of *i.v.* injection of Mamb-1 on basal paw mechanical threshold in naive rats (Suppl. Fig. 1), the *i.v.* injection of Mamb-1 30 minutes before the first *i.p.* injection of ISDN did not change the basal face and paw mechanical sensitivities (Fig. 5A, B, black symbols). The acute effect of ISDN, with the maximal allodynia reaching 5.3 ± 0.5 from the basal level of 8.2 ± 0.2g on the face, and 13.7 ± 0.3 from a basal level of 18.5 ± 0.2g on the paw (Fig. 5A, B black symbols) after two hours, was not significantly different from the one of vehicle injected rats (Fig. 5C, D black symbols). A basal allodynia appeared the day after (*i.e.*, on day 2; Fig 5E, F) that was reversed by Mamb-1 *i.v.* injected 30 minutes before the second ISDN injection (Fig. 5A, B red symbols), whereas vehicle was without effect (Fig. 5C, D, red symbols). On day 3, the basal cutaneous allodynia was significantly less pronounced in Mamb-1-treated compared to vehicle-treated rats, reaching 5.1 ± 0.4g on the face and 14.7 ± 0.3g on the paw, and 2.9 ± 0.4g on the face and 13.4 ± 0.2g on the paw, respectively (Fig. 5E, F). Repeated *i.v.* injection of Mamb-1 on day 3 and 4 finally led to a significant reduction in the maximal chronic allodynia on day 5, *i.e.,* 24 hours after the last ISDN injection, reaching 4.7 ± 0.3g on face and 13.8 ± 0.5g on paw, compared to 1.9 ± 0.3g and 11.5 ± 0.4g, respectively, on vehicle-treated rats (Fig. 5E, F). Consequently, an ISDN-induced acute increase in allodynia was still observed in Mamb-1-treated rats on the fourth day (Fig. 5A, B, blue symbols), but not in vehicle-treated rats already close to the maximal allodynic level (Fig. 5C, D, blue symbols).

Our results show that daily inter-attack *i.v.* injection of Mamb-1 was able to significantly reduce the chronic allodynia that develops upon injection of ISDN for several days, especially on facial territory, without affecting normal cutaneous sensitivity nor the ability of ISDN to induce an acute allodynic effect. The absence of preventive effect of Mamb-1 *i.v.* injected 30 min before the first ISDN injection could be due to a limited half-life of Mamb-1 in blood circulation regarding the 30 to 90 min needed after ISDN injection (i.e. 60 to 120 min after Mamb-1 injection) for allodynia to develop (Suppl. Fig.2).

The anti-allodynic effect of *i.v.* mambalgin-1 in the ISDN-induced chronic migraine model is still present in ASIC1a knock-out mice

Since Mamb-1 inhibits ASIC1-containing channels (*i.e.*, comprising either ASIC1a- and/or ASIC1b subunits), the contribution of ASIC1a to its anti-allodynic effects in the ISDN-induced chronic migraine model was tested on hindpaw mechanical sensitivity in ASIC1a-knock-out (KO) mice. In wild-type mice, the first *i.p.* injection of ISDN induced an acute paw allodynia, with the withdrawal force decreasing from 4.1 ± 0.1 down to 3.0 ± 0.1g two hours after the ISDN injection (Fig. 6A, black symbols). Allodynia was not fully reversed the next day, and one ISDN injection per day during four days resulted, like in rats, in the progressive development of a chronic mechanical allodynia correlated with a progressive decrease in the daily total effect of ISDN, leading to the absence of effect of the fourth ISDN injection (Fig. 6A, blue symbols). On day 5 (*i.e.*, 24 hours after the last ISDN injection), the maximal chronic allodynia reaches 2.7 ± 0.1 from the control (day 1) value of 4.1 ± 0.1g and was reversed towards control mechanical sensitivity by an *i.v.* injection of Mamb-1 (Fig. 6B). Interestingly, the reversion of chronic paw allodynia was complete in mice, whereas only partial in rats. The same experiments have been done in ASIC1a-KO mice and showed no difference with wild-type animals either in the ISDN-induced acute allodynia (at day 1 and at day 4) (Fig. 6C), nor in the development of chronic allodynia (reaching 2.6 ± 0.1 from the control day 1 value of 4.1 ± 0.1g, not significantly different from wild-type mice with Mann Whitney non parametric test) and in the anti-allodynic effects of *i.v.* Mamb-1 on the maximal chronic allodynia (Fig. 6D).

These data show that ASIC1a is not needed for the anti-allodynic effects of Mamb-1 nor for establishment of the ISDN-induced migraine model in mice. They also indicate that ISDN has a similar effect in mice than in rats after repetitive daily injections with the establishment of a maximal chronic basal allodynia, which is consistent with what was previously described with nitroglycerin as the NO-donor (Pradhan *et al.*, 2014).

Discussion

In this study, we show the anti-allodynic effects of intravenous ASIC1 inhibitors in a rodent model of migraine induced by daily *i.p.* injection of ISDN, a long lasting NO-donor. Mambalgin-1 and amiloride reverse cephalic and extra-cephalic cutaneous allodynia when *i.v.* injected during the attack-like acute effect of one ISDN injection, with an effect similar to

the one of sumatriptan, and cause a delay in the establishment of chronic allodynia induced by subsequent ISDN injections. ASIC1 inhibitors are also able to reverse the maximal cephalic and extra-cephalic chronic allodynia when *i.v.* injected after the four injections of ISDN, with an effect similar to the one of topiramate. Daily inter-attack *i.v.* injection of Mamb-1 is able to significantly reduce maximal cutaneous allodynia, thus exerting a preventive effect on the establishment of chronic allodynia.

Involvement of peripheral ASIC1-containing channels in migraine-induced cutaneous allodynia and in its chronification.

The contribution of ASIC1 channels in acute and chronic cutaneous allodynia in the ISDN-induced migraine model is strongly supported by the similar anti-allodynic effects of amiloride, a well described non-selective inhibitor of ASICs, and Mamb-1, a specific inhibitor of ASIC1-containing channels (Diochot *et al.*, 2012). Mamb-1, contrary to amiloride, does not block the epithelial sodium channel involved in blood pressure regulation (Suppl. Fig. 4), making unlikely a significant indirect vascular contribution of these compounds in the ISDN-induced migraine model. In rodents, Mamb-1 only inhibits ASIC1a- and ASIC1b-containing channels, with ASIC1a expressed in both central and sensory neurons (small diameter neurons), and ASIC1b exclusively expressed in sensory neurons (small to large diameter neurons) (Chen *et al.*, 1998). We have previously shown that the central effects of Mamb-1 are totally lost in ASIC1a-KO mice (Diochot *et al.*, 2012; Diochot *et al.*, 2016). ASIC1a is not necessary to the anti-allodynic effect of *i.v.* Mamb-1 in the ISDN-induced migraine model. This precludes a major contribution of central ASIC1a-containing channels and supports a peripheral effect involving ASIC1b specifically expressed in sensory neurons, although a direct demonstration would need genetic ablation of ASIC1b in TG neuron. However, native ASICs are composed of three identical or different subunits, and the contribution of peripheral ASIC1a subunit in wild-type animals cannot be ruled out, for instance within heteromeric channels made of ASIC1a and ASIC1b. Our results are also in good agreement with our previous data in mice showing a major role for peripheral ASIC1b-containing channels in the analgesic effect of *i.v.* mambalgin-1 on inflammatory pain (Diochot *et al.*, 2016).

Peripheral ASIC1-containing channels in TG sensory fibers could be therefore involved in the pathophysiology of migraine, possibly correlated with meningeal extracellular acidification as one of the initiating events. Our results support the involvement of ASICs that can be activated by NO-induced extracellular acidification (through mast cells

degranulation) and further stimulated by inflammatory mediators and associated transduction pathways. ASIC1- and ASIC3-containing channels were proposed as important pain detectors in sensory neurons of the orofacial area (Fu *et al.*, 2016) notably in the dura mater (Yan *et al.*, 2011; Yan *et al.*, 2013; Burgos-Vega *et al.*, 2015). About 80% of rat dural afferents trigger action potentials at pH6.0, 50% at pH7.0 and 30% at pH7.1. As a consequence, an acidic pH6.0 solution applied on dura-mater generates sustained cephalic and extra-cephalic allodynia, which is maximal after 2 hours and inhibited by amiloride but not TRPV1 antagonists, supporting the involvement of ASICs activation in migraine-related behavior *in vivo* (Yan *et al.*, 2011; Yan *et al.*, 2013). ASIC3-containing channels have been proposed to be involved in these effects (Yan *et al.*, 2013), as well as in the potentiating effects of inflammatory factors, but our data now also support the involvement of ASIC1-containing channels (presumably ASIC1b) since Mamb-1 does not inhibit ASIC3-containing channels (Diochot *et al.*, 2012). Interestingly, Mamb-1 was shown to modify the pH-dependent activation and inactivation curves of ASIC1a channels (Diochot *et al.*, 2012; Salinas *et al.*, 2014) with a higher inhibitory potency in conditions of mild acidosis (are thought to happen around sensory nerves terminals in pathological conditions such as inflammation or migraine triggering. In addition to ASIC3-containing channels, which are expressed in 80% of pH-sensitive dural fibers (Yan *et al.*, 2013), the ASIC1a, ASIC1b and ASIC2 subunits were also present in TG neurons (Manteniotis *et al.*, 2013; Cho *et al.*, 2015; Flegel *et al.*, 2015; Fu *et al.*, 2016), and data obtained with ASIC1a-KO mice support the involvement of ASIC1-like currents in TG ganglion in orofacial inflammatory pain (Fu *et al.*, 2016). Transcriptome analyses recently showed higher expression of ASIC1 in TG versus lumbar DRG neurons (Lopes *et al.*, 2017). Another interesting point concerns the NO potentiation of ASICs in heterologous systems as well as in rat sensory neurons (Cadiou *et al.*, 2007), with transient effects on ASIC1a, ASIC2a and ASIC3 currents, but an irreversible effect on rat ASIC1b current that could also contribute to the role of ASIC1b in the ISDN-induced model.

Inhibition of peripheral ASIC1-containing channels in TG afferents by systemic Mamb-1 and amiloride could thus participate in the analgesic effects seen in the ISDN-induced rat migraine model. Local *i.pl.* injection of Mamb-1 in the paw was not able to reverse ISDN-induced chronic paw mechanical allodynia, whereas it fully reversed the inflammatory-induced one. The systemic extra-cephalic, anti-allodynic effect of *i.v.* Mamb-1 would thus not be due to local inhibition of peripheral sensory ASIC1-containing channels in the paw, but would rather be a consequence of the reversion of cephalic ISDN-induced

allodynia through inhibition of ASIC1-containing channels in TG sensory fibers. Peripheral sensitization of the TG sensory neurons leads to secondary central sensitization of the second order neurons of the TNC and upper cervical spinal cord (C1-C2), thus causing subsequent cephalic allodynia, whereas extra-cephalic allodynia would reflect the further extension of central sensitization to upper central pain relays (like thalamus), particularly during the settlement of a chronic state (Boyer *et al.*, 2014). Highly diffusible NO is also able to directly exert central effects, with modulation of medullary dorsal horn neurons (Flores Ramos *et al.*, 2017), TNC neurons, and VPM thalamus neurons (Goadsby *et al.*, 2017), thus amplifying cutaneous pain sensitization. The anti-allodynic and anti-chronification effects of ASIC1 inhibitors are weaker on extra-cephalic than on cephalic allodynia in our experiments in rats. Similar incomplete effects were reported for amiloride in another rat migraine model with a direct dural acidic stimulation (Yan *et al.*, 2013) and in a mice NTG-induced model of chronic migraine (Tipton *et al.*, 2016), cephalic allodynia being not assessed in both studies. The complete reversibility of cephalic allodynia by ASIC1 inhibitors that we observed would suggest that sensitization of the TNC and the upper cervical dorsal horn could depend directly on the activity of TG sensory neurons expressing ASIC1-containing channels, whereas extra-cephalic allodynia would be partially independent of them, involving central mechanisms independent of TG fibers activation (Bernstein & Burstein, 2012) or ASIC-independent effects of NO on paw sensory fibers (Ferrari *et al.*, 2016).

Systemic ASIC1 blockers against migraine

Treatment of migraine, and particularly chronic migraine, remains challenging, and numerous therapeutic drugs are non specific, sometimes inefficient, with numerous side effects and contra-indications (Serrano *et al.*, 2015; Schytz *et al.*, 2017). Cutaneous allodynia in chronic migraine is associated with inadequate outcomes for any anti-migraine medication (Lipton *et al.*, 2017). Furthermore, a significant proportion of chronic migraine cases are due to anti-migraine medication abuse or misuse (Bigal & Lipton, 2009; Lipton *et al.*, 2015), highlighting the need of new medications, including new prophylactic approaches to prevent the chronification process.

We show that *i.v.* amiloride and mambalgin-1 both exert long-lasting anti-allodynic effects against acute and chronic cutaneous allodynia in the ISDN-induced migraine model, not only in extra-cephalic territories as usually assessed but also in cephalic ones, and that *i.v.* mambalgin-1 is able to exert a prophylactic effect on the development of chronic allodynia,

without affecting normal cutaneous sensitivity. This supports systemic (among which orally administrated) ASIC1 inhibitors as new potential therapeutic leads against migraine and headaches and this is in good agreement with data showing that a preventive daily therapy with *i.p.* amiloride in mice partially reduce acute NTG-induced as well as chronic basal mechanical paw hypersensitivity (Tipton *et al.*, 2016). A pilot open clinical study has also shown that systemic treatment with amiloride reduced aura and headache symptoms in four of seven patients with intractable aura (Holland *et al.*, 2012). Drawback of amiloride, which is used in humans as a diuretic and antihypertensive, is a poor specificity, and our data suggest that more specific ASIC1 blockers like mambalgin-1 could also be used 1) to relieve migraine attack, with benefits on subsequent chronification, 2) to relieve established chronic allodynia, and 3) as a preventive treatment against chronification.

References

Alexander SP, Peters JA, Kelly E, Marrion NV, Faccenda E, Harding SD, *et al.* (2017). THE CONCISE GUIDE TO PHARMACOLOGY 2017/18: Ligand-gated ion channels. Br J Pharmacol 174 Suppl 1**:** S130-S159.

Ashina M, Hansen JM, & Olesen J (2013). Pearls and pitfalls in human pharmacological models of migraine: 30 years' experience. Cephalalgia 33**:** 540-553.

Baron A, Diochot S, Salinas M, Deval E, Noel J, & Lingueglia E (2013). Venom toxins in the exploration of molecular, physiological and pathophysiological functions of acid-sensing ion channels. Toxicon 75**:** 187-204.

Bates EA, Nikai T, Brennan KC, Fu YH, Charles AC, Basbaum AI, *et al.* (2010). Sumatriptan alleviates nitroglycerin-induced mechanical and thermal allodynia in mice. Cephalalgia 30**:** 170-178.

Bernstein C, & Burstein R (2012). Sensitization of the trigeminovascular pathway: perspective and implications to migraine pathophysiology. J Clin Neurol 8**:** 89-99.

Besson T, Lingueglia E, & Salinas M (2017). Pharmacological modulation of Acid-Sensing Ion Channels 1a and 3 by amiloride and 2-guanidine-4-methylquinazoline (GMQ). Neuropharmacology 125**:** 429-440.

Bigal ME, & Lipton RB (2009). Overuse of acute migraine medications and migraine chronification. Curr Pain Headache Rep 13**:** 301-307.

Bigal ME, Serrano D, Buse D, Scher A, Stewart WF, & Lipton RB (2008). Acute migraine medications and evolution from episodic to chronic migraine: a longitudinal population-based study. Headache 48**:** 1157-1168.

Bohlen CJ, Chesler AT, Sharif-Naeini R, Medzihradszky KF, Zhou S, King D, *et al.* (2011). A heteromeric Texas coral snake toxin targets acid-sensing ion channels to produce pain. Nature 479**:** 410-414.

Boyer N, Dallel R, Artola A, & Monconduit L (2014). General trigeminospinal central sensitization and impaired descending pain inhibitory controls contribute to migraine progression. Pain 155**:** 1196-1205.

Burgos-Vega C, Moy J, & Dussor G (2015). Meningeal afferent signaling and the pathophysiology of migraine. Prog Mol Biol Transl Sci 131**:** 537-564.

Burstein R, Jakubowski M, Garcia-Nicas E, Kainz V, Bajwa Z, Hargreaves R, *et al.* (2010). Thalamic sensitization transforms localized pain into widespread allodynia. Ann Neurol 68**:** 81-91.

Cadiou H, Studer M, Jones NG, Smith ES, Ballard A, McMahon SB, *et al.* (2007). Modulation of acid-sensing ion channel activity by nitric oxide. J Neurosci 27**:** 13251-13260.

Chen CC, England S, Akopian AN, & Wood JN (1998). A sensory neuron-specific, proton-gated ion channel. Proc Natl Acad Sci U S A 95**:** 10240-10245.

Cho JH, Choi IS, Nakamura M, Lee SH, Lee MG, & Jang IS (2015). Proton-induced currents in substantia gelatinosa neurons of the rat trigeminal subnucleus caudalis. Eur J Pharmacol 762**:** 18-25.

Dallel R, Descheemaeker A, & Luccarini P (2018). Recurrent administration of the nitric oxide donor, isosorbide dinitrate, induces a persistent cephalic cutaneous hypersensitivity: A model for migraine progression. Cephalalgia 38**:** 776-785.

Deval E, & Lingueglia E (2015). Acid-Sensing Ion Channels and nociception in the peripheral and central nervous systems. Neuropharmacology 94**:** 49-57.

Deval E, Noel J, Lay N, Alloui A, Diochot S, Friend V, *et al.* (2008). ASIC3, a sensor of acidic and primary inflammatory pain. EMBO J 27**:** 3047-3055.

Diochot S, Alloui A, Rodrigues P, Dauvois M, Friend V, Aissouni Y, *et al.* (2016). Analgesic effects of mambalgin peptide inhibitors of acid-sensing ion channels in inflammatory and neuropathic pain. Pain 157**:** 552-559.

Diochot S, Baron A, Salinas M, Douguet D, Scarzello S, Dabert-Gay AS, *et al.* (2012). Black mamba venom peptides target acid-sensing ion channels to abolish pain. Nature 490**:** 552-555.

Dussor G (2015). ASICs as therapeutic targets for migraine. Neuropharmacology 94**:** 64-71.

Edelmayer RM, Vanderah TW, Majuta L, Zhang ET, Fioravanti B, De Felice M, *et al.* (2009). Medullary pain facilitating neurons mediate allodynia in headache-related pain. Ann Neurol 65**:** 184-193.

Farkas S, Bolcskei K, Markovics A, Varga A, Kis-Varga A, Kormos V, *et al.* (2016). Utility of different outcome measures for the nitroglycerin model of migraine in mice. J Pharmacol Toxicol Methods 77**:** 33-44.

Ferrari LF, Levine JD, & Green PG (2016). Mechanisms mediating nitroglycerin-induced delayed-onset hyperalgesia in the rat. Neuroscience 317**:** 121-129.

Flegel C, Schobel N, Altmuller J, Becker C, Tannapfel A, Hatt H, *et al.* (2015). RNA-Seq Analysis of Human Trigeminal and Dorsal Root Ganglia with a Focus on Chemoreceptors. PLoS One 10**:** e0128951.

Flores Ramos JM, Devoize L, Descheemaeker A, Molat JL, Luccarini P, & Dallel R (2017). The nitric oxide donor, isosorbide dinitrate, induces a cephalic cutaneous hypersensitivity, associated with sensitization of the medullary dorsal horn. Neuroscience 344**:** 157-166.

Fu H, Fang P, Zhou HY, Zhou J, Yu XW, Ni M, *et al.* (2016). Acid-sensing ion channels in trigeminal ganglion neurons innervating the orofacial region contribute to orofacial inflammatory pain. Clin Exp Pharmacol Physiol 43**:** 193-202.

Goadsby PJ, Holland PR, Martins-Oliveira M, Hoffmann J, Schankin C, & Akerman S (2017). Pathophysiology of Migraine: A Disorder of Sensory Processing. Physiol Rev 97**:** 553-622.

Hansen EK, & Olesen J (2017). Towards a pragmatic human migraine model for drug testing: 2. Isosorbide-5-mononitrate in healthy individuals. Cephalalgia 37**:** 11-19.

Harding SD, Sharman JL, Faccenda E, Southan C, Pawson AJ, Ireland S, *et al.* (2018). The IUPHAR/BPS Guide to PHARMACOLOGY in 2018: updates and expansion to encompass the new guide to IMMUNOPHARMACOLOGY. Nucleic Acids Res 46**:** D1091-D1106.

Harris HM, Carpenter JM, Black JR, Smitherman TA, & Sufka KJ (2017). The effects of repeated nitroglycerin administrations in rats; modeling migraine-related endpoints and chronification. J Neurosci Methods 284**:** 63-70.

Holland PR, Akerman S, Andreou AP, Karsan N, Wemmie JA, & Goadsby PJ (2012). Acid-sensing ion channel 1: a novel therapeutic target for migraine with aura. Ann Neurol 72**:** 559-563.

Iversen HK, Nielsen TH, Garre K, Tfelt-Hansen P, & Olesen J (1992). Dose-dependent headache response and dilatation of limb and extracranial arteries after three doses of 5-isosorbide-mononitrate. Eur J Clin Pharmacol 42**:** 31-35.

Jansen-Olesen I, Tfelt-Hansen P, & Olesen J (2013). Animal migraine models for drug development: status and future perspectives. CNS Drugs 27**:** 1049-1068.

Karatas H, Erdener SE, Gursoy-Ozdemir Y, Lule S, Eren-Kocak E, Sen ZD, *et al.* (2013). Spreading depression triggers headache by activating neuronal Panx1 channels. Science 339**:** 1092-1095.

Kilkenny C, Browne W, Cuthill IC, Emerson M, & Altman DG (2010). Animal research: reporting in vivo experiments: the ARRIVE guidelines. Br J Pharmacol 160**:** 1577-1579.

Levy D (2009). Migraine pain, meningeal inflammation, and mast cells. Curr Pain Headache Rep 13**:** 237-240.

Lipton RB, Bigal ME, Ashina S, Burstein R, Silberstein S, Reed ML, *et al.* (2008). Cutaneous allodynia in the migraine population. Ann Neurol 63**:** 148-158.

Lipton RB, Fanning KM, Serrano D, Reed ML, Cady R, & Buse DC (2015). Ineffective acute treatment of episodic migraine is associated with new-onset chronic migraine. Neurology 84**:** 688-695.

Lipton RB, Munjal S, Buse DC, Bennett A, Fanning KM, Burstein R, *et al.* (2017). Allodynia Is Associated With Initial and Sustained Response to Acute Migraine Treatment: Results from the American Migraine Prevalence and Prevention Study. Headache 57**:** 1026-1040.

Lopes DM, Denk F, & McMahon SB (2017). The molecular fingerprint of dorsal root and trigeminal ganglion neurons. Frontiers in Molecular Neuroscience 10**:** 1-11.

Louter MA, Bosker JE, van Oosterhout WP, van Zwet EW, Zitman FG, Ferrari MD, *et al.* (2013). Cutaneous allodynia as a predictor of migraine chronification. Brain 136**:** 3489-3496.

Manteniotis S, Lehmann R, Flegel C, Vogel F, Hofreuter A, Schreiner BS, *et al.* (2013). Comprehensive RNA-Seq expression analysis of sensory ganglia with a focus on ion channels and GPCRs in Trigeminal ganglia. PLoS One 8**:** e79523.

Marra S, Ferru-Clement R, Breuil V, Delaunay A, Christin M, Friend V, *et al.* (2016). Non-acidic activation of pain-related Acid-Sensing Ion Channel 3 by lipids. EMBO J 35**:** 414-428.

Mazzuca M, Heurteaux C, Alloui A, Diochot S, Baron A, Voilley N, *et al.* (2007). A tarantula peptide against pain via ASIC1a channels and opioid mechanisms. Nat Neurosci 10**:** 943-945.

McGrath JC, & Lilley E (2015). Implementing guidelines on reporting research using animals (ARRIVE etc.): new requirements for publication in BJP. Br J Pharmacol 172**:** 3189-3193.

Mourier G, Salinas M, Kessler P, Stura EA, Leblanc M, Tepshi L, *et al.* (2016). Mambalgin-1 Pain-relieving Peptide, Stepwise Solid-phase Synthesis, Crystal Structure, and Functional Domain for Acid-sensing Ion Channel 1a Inhibition. J Biol Chem 291**:** 2616-2629.

Nahman-Averbuch H, Shefi T, Schneider VJ, 2nd, Li D, Ding L, King CD, *et al.* (2018). Quantitative sensory testing in patients with migraine: a systematic review and meta-analysis. Pain 159**:** 1202-1223.

Olesen J, & Ashina M (2015). Can nitric oxide induce migraine in normal individuals? Cephalalgia 35**:** 1125-1129.

Pradhan AA, Smith ML, McGuire B, Tarash I, Evans CJ, & Charles A (2014). Characterization of a novel model of chronic migraine. Pain 155**:** 269-274.

Rozniecki JJ, Dimitriadou V, Lambracht-Hall M, Pang X, & Theoharides TC (1999). Morphological and functional demonstration of rat dura mater mast cell-neuron interactions in vitro and in vivo. Brain Res 849**:** 1-15.

Salinas M, Besson T, Delettre Q, Diochot S, Boulakirba S, Douguet D, *et al.* (2014). Binding site and inhibitory mechanism of the mambalgin-2 pain-relieving peptide on acid-sensing ion channel 1a. J Biol Chem 289**:** 13363-13373.

Scher AI, Buse DC, Fanning KM, Kelly AM, Franznick DA, Adams AM, *et al.* (2017). Comorbid pain and migraine chronicity: The Chronic Migraine Epidemiology and Outcomes Study. Neurology 89**:** 461-468.

Schytz HW, Hargreaves R, & Ashina M (2017). Challenges in developing drugs for primary headaches. Prog Neurobiol 152**:** 70-88.

Serrano D, Buse DC, Manack Adams A, Reed ML, & Lipton RB (2015). Acute treatment optimization in episodic and chronic migraine: results of the American Migraine Prevalence and Prevention (AMPP) Study. Headache 55**:** 502-518.

Thomsen LL, Brennum J, Iversen HK, & Olesen J (1996). Effect of a nitric oxide donor (glyceryl trinitrate) on nociceptive thresholds in man. Cephalalgia 16**:** 169-174.

Tipton AF, Tarash I, McGuire B, Charles A, & Pradhan AA (2016). The effects of acute and preventive migraine therapies in a mouse model of chronic migraine. Cephalalgia 36**:** 1048-1056.

Vos T, Allen C, Arora M, Barber RM, Bhutta ZA, Brown A, *et al.* (2016). Global, regional, and national incidence, prevalence, and years lived with disability for 310 diseases and injuries, 1990-2015: a systematic analysis for the Global Burden of Disease Study 2015. GBD 2015 Disease and Injury Incidence and Prevalence Collaborators. Lancet 388**:** 1545-1602.

Waldmann R, Champigny G, Bassilana F, Heurteaux C, & Lazdunski M (1997). A proton-gated cation channel involved in acid-sensing. Nature 386**:** 173-177.

Wemmie JA, Chen J, Askwith CC, Hruska-Hageman AM, Price MP, Nolan BC, *et al.* (2002). The acid-activated ion channel ASIC contributes to synaptic plasticity, learning, and memory. Neuron 34**:** 463-477.

Yan J, Edelmayer RM, Wei X, De Felice M, Porreca F, & Dussor G (2011). Dural afferents express acid-sensing ion channels: a role for decreased meningeal pH in migraine headache. Pain 152**:** 106-113.

Yan J, Wei X, Bischoff C, Edelmayer RM, & Dussor G (2013). pH-evoked dural afferent signaling is mediated by ASIC3 and is sensitized by mast cell mediators. Headache 53**:** 1250-1261.

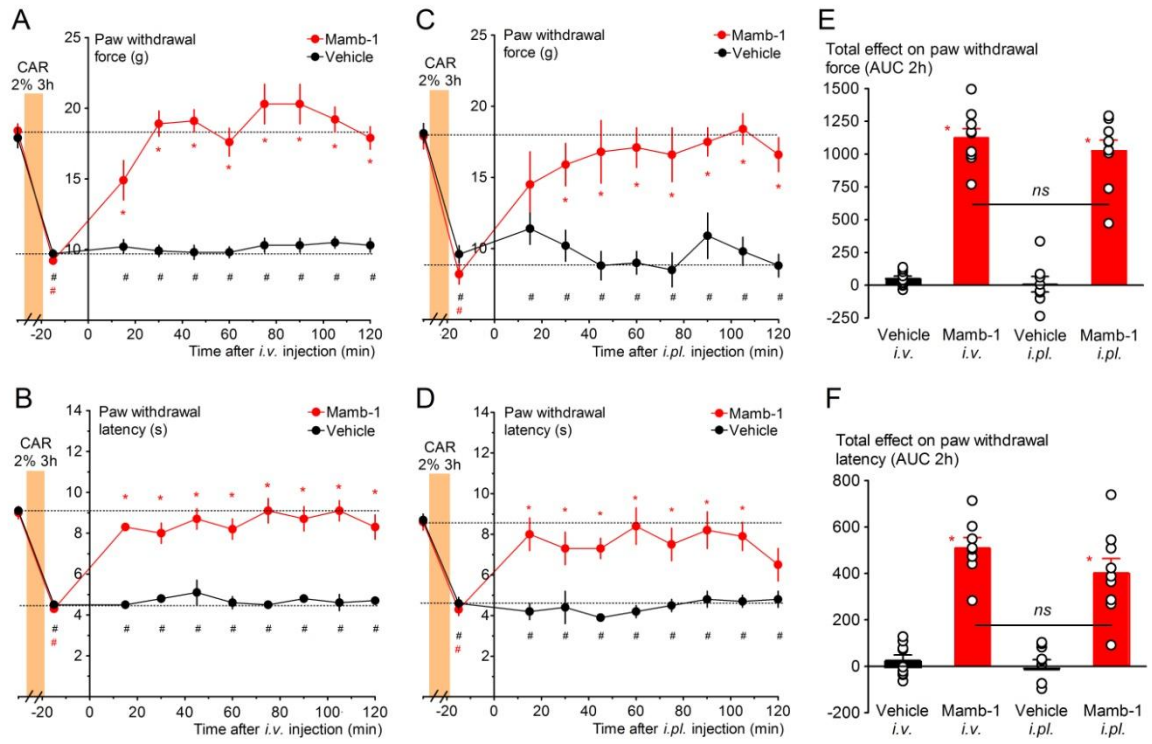

Fig. 1: Reversion of inflammation-induced paw mechanical allodynia and thermal hyperalgesia by intravenous and local intraplantar injections of mambalgin-1 in rats.

A, C -Full reversion by *i.v.* (**A**) and by *i.pl.* (**C**) Mamb-1 (11.3 and 6.7 nmol/kg, respectively) of paw inflammatory mechanical allodynia (carrageenan 2%, 3h). **B, D** - Full reversion by *i.v.* (**B**) and *i.pl.* (**D**) Mamb-1 of paw inflammatory thermal hyperalgesia (carrageenan 2%, 3h). A-D, Mean ± SEM, n=9, respectively. * $p<0.05$ compared to vehicle with Mann Whitney non parametric test, # $p<0.05$ compared to control non inflamed basal value with Wilcoxon matched paired test.. **E, F** -Total effect of *i.v.* and of *i.pl.* Mamb-1 on paw mechanical withdrawal force calculated as the Area Under Curve (AUC) (**E**) and on heat paw withdrawal latency (**F**) calculated as the AUC during 2 hours after the injection. Individual dat points and mean ± SEM n=9, * $p<0.05$ compared to vehicle with Mann Whitney non parametric test.

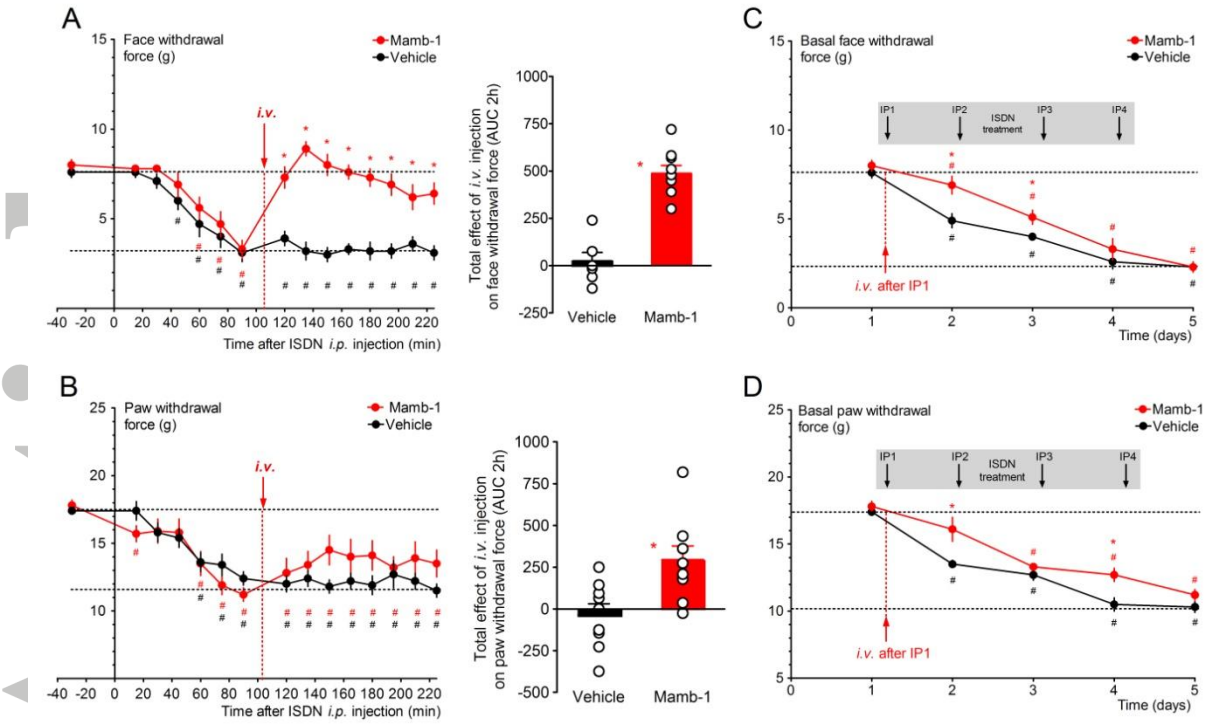

Fig. 2: Reversion of ISDN-induced cephalic and extra-cephalic acute mechanical allodynia by an intravenous injection of mambalgin-1.

A, B - Left panels - Kinetics of the anti-allodynic effect on face (**A**) and paw (**B**) mechanical withdrawal thresholds (g) of an *i.v.* injection of Mamb-1 (11.3 nmol/kg) 105 minutes after the *i.p.* injection of ISDN in rats. Mean ± SEM, n = 9: * $p<0.05$ compared to vehicle with Mann Whitney non parametric test; # $p<0.05$ compared to control value before ISDN injection with Wilcoxon matched paired test. **Right panels** - Total effect of *i.v.* Mamb-1 (or vehicle) on face (**A**) and paw (**B**) withdrawal force calculated as the Area Under Curve (AUC) during 2 hours after the *i.v.* injection. Individual data points and mean ± SEM, n = 9, * $p<0.05$ compared to vehicle with Mann Whitney non parametric test. **C, D** - One *i.v.* injection of Mamb-1 (11.3 nmol/kg) after the first ISDN injection, as shown in **A** and **B**, induces a delay in the subsequent settlement of ISDN-induced chronic allodynia induced by three more daily ISDN injections. Basal face (**C**) and paw (**D**) mechanical withdrawal force (g) measured before each daily ISDN injection and the day after the last ISDN injection (day 5). Mean ± SEM, n = 9: * $p<0.05$ compared to vehicle with Mann Whitney non parametric test; # $p<0.05$ compared to control before the first ISDN injection with Wilcoxon matched paired test.

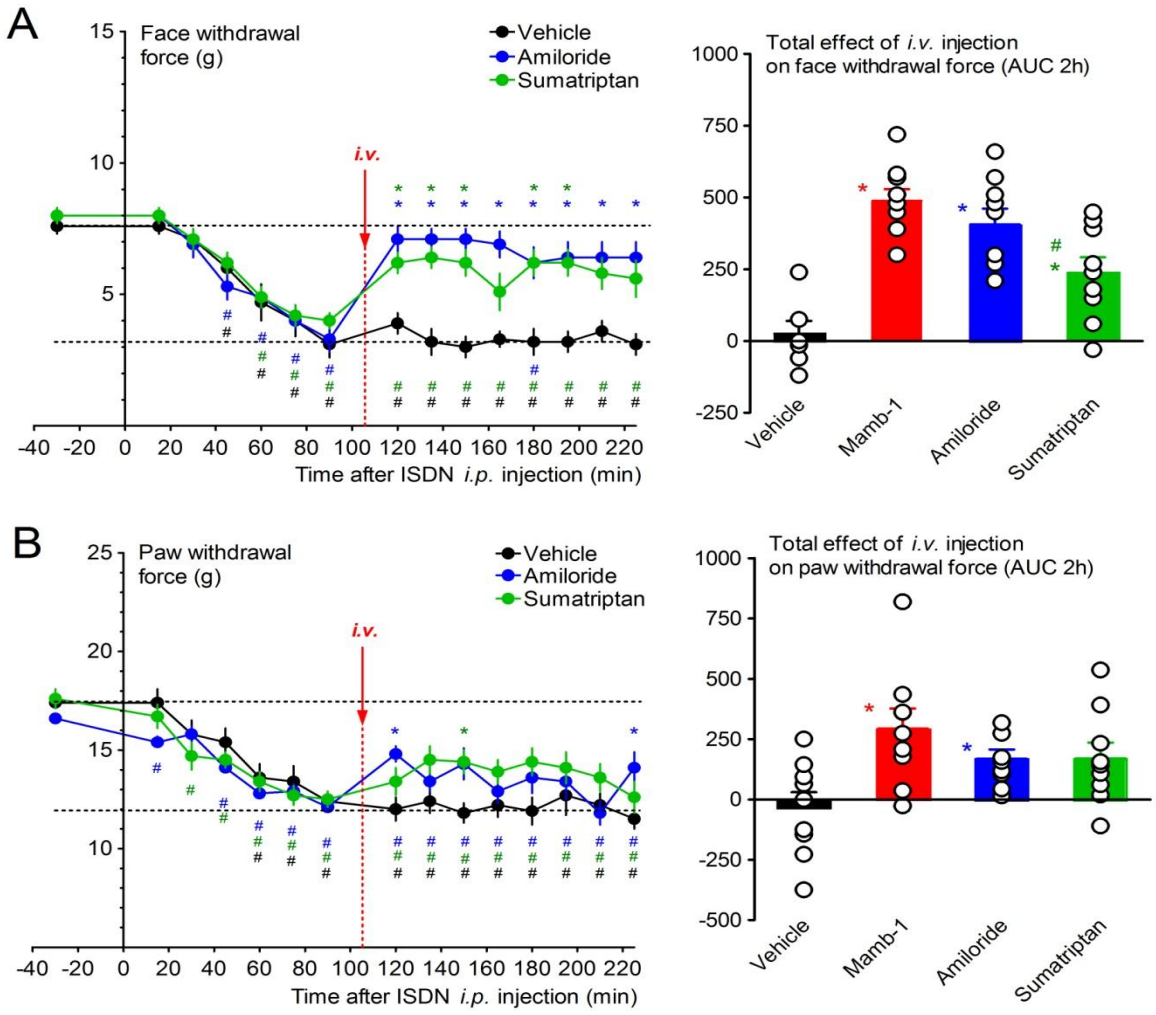

Fig. 3: Comparison of the anti-allodynic effects of mambalgin-1, amiloride and sumatriptan on ISDN-induced cephalic and extra-cephalic acute mechanical allodynia.

A, B Left panels - Kinetics of the analgesic effects on face (**A**) and paw (**B**) mechanical withdrawal force (g) of amiloride (10 mg/kg) and sumatriptan succinate (Imiject©, 10 mg/kg) *i.v.* injected 105 minutes after the injection of ISDN measured on the same rats. Mean ± SEM, n = 9. * $p<0.05$ with non-parametric Kruskal-Wallis and Dunn's post hoc tests compared to vehicle; # $p<0.05$ with Wilcoxon matched paired test compared to control value before ISDN injection. For clarity, only vehicle (same data as in Fig. 2A, B) but not Mamb-1 is shown. **Right panels** - Total effect of vehicle, Mamb-1 (same data as in Fig. 2A, B), amiloride and sumatriptan on face (**A**) and paw (**B**) withdrawal force calculated as the Area Under Curve (AUC) during 2 hours after injection. Individual data points and mean ± SEM, n = 9: * $p<0.05$ with Mann Whitney non parametric test compared to vehicle; # $p<0.05$ with Mann Whitney non parametric test compared to Mamb-1.

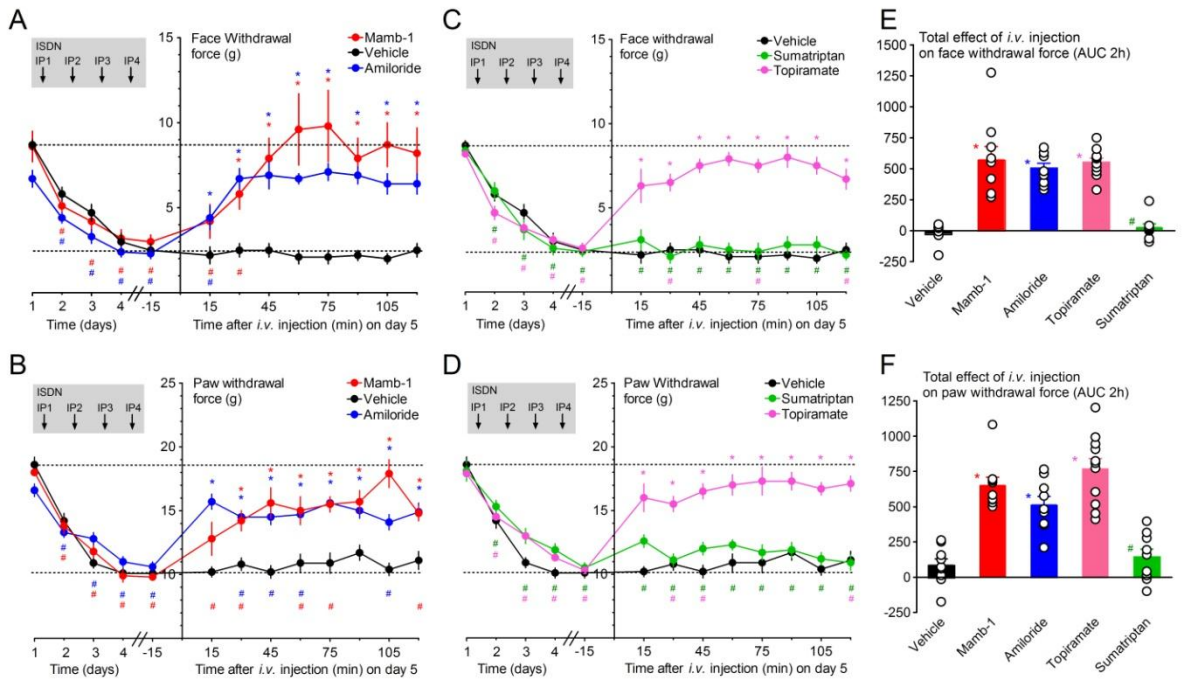

Fig. 4: Reversion of ISDN-induced maximal cephalic and extra-cephalic chronic mechanical allodynia by an intravenous injection of mambalgin-1.

A-D - Kinetics of the anti-allodynic effect of Mamb-1 (11.3 nmol/kg), amiloride (10 mg/kg), sumatriptan succinate (Imiject©, 10 mg/kg) and topiramate (30 mg/kg), *i.v.* injected one day after the last ISDN injection (*i.e.*, on day 5) on face (**A, C**) and paw (**B, D**) mechanical withdrawal force (g) in rats. The basal mechanical withdrawal force (g) was measured before each daily ISDN injection (left side of the y axe), showing the chronification process of cutaneous allodynia day after day. For clarity, kinetics were split into two graphs, sharing the same data for vehicle. Mean ± SEM, n = 9 except with topiramate (n=11). * $p<0.05$ with Mann Whitney non parametric test compared to vehicle; # $p<0.05$ with Wilcoxon matched paired test compared to control value before the first ISDN injection (day 1), not shown but all significant for vehicle. **E, F** - Total effect on face (**E**) and paw (**F**) withdrawal force calculated as the Area Under Curve (AUC) during 2 hours after the *i.v.* injection for each rat. Individual data points and mean ± SEM n = 9: * $p<0.05$ with Mann Whitney non parametric test compared to vehicle; # $p<0.05$ with Mann Whitney non parametric test compared to Mamb-1.

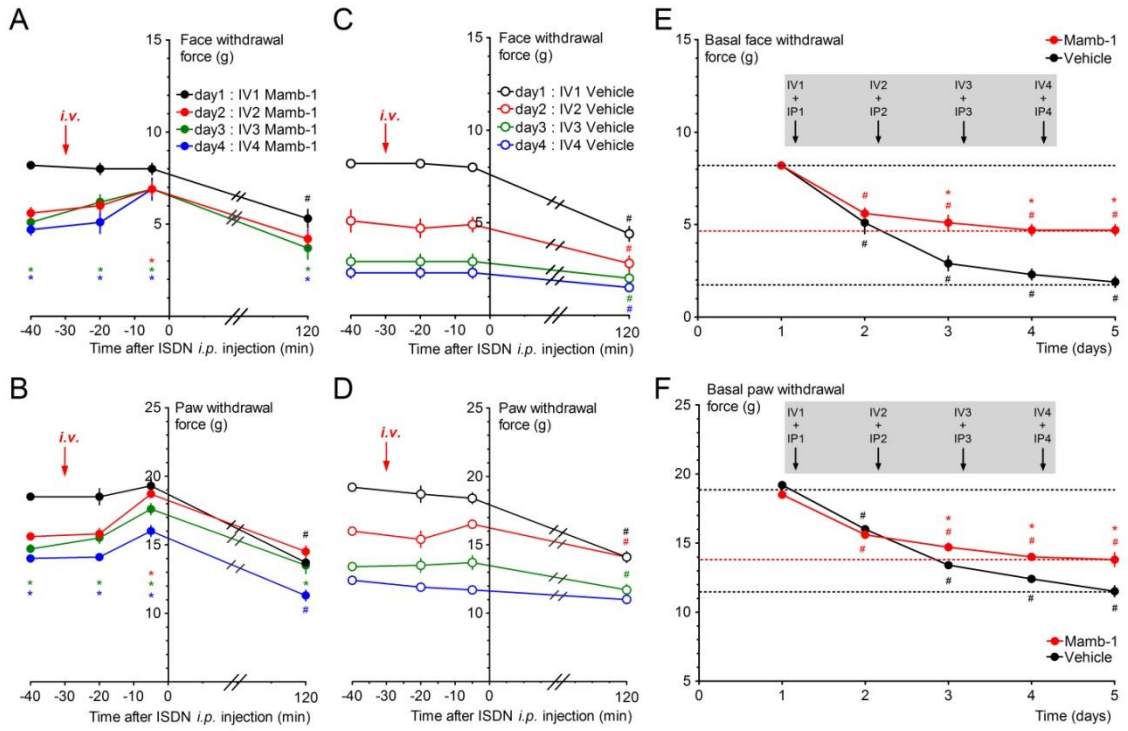

Fig. 5: Preventive effect of *i.v.* Mamb-1 treatment on chronification of cephalic and extra-cephalic mechanical allodynia.

A-D - Kinetics of the effects of a daily *i.v.* injection of Mamb-1 (11.3 nmol/kg, **A, B**) or vehicle (**C, D**) 30 min before each daily ISDN injection (10 mg/kg) on face (**A, C**) and paw (**B, D**) mechanical withdrawal threshold (g). Mean ± SEM, n = 9: * $p<0.05$ with Mann Whitney non parametric test compared to vehicle; # $p<0.05$ with Wilcoxon matched paired test compared to baseline value before any injection. **E, F** - Effects of a daily *i.v.* injection of Mamb-1 or vehicle (same conditions as in A-D) on the basal face (**E**) and paw (**F**) mechanical withdrawal force threshold (g) measured on the same rats before each daily *i.v.* injections (values at time -40 on graphs A-D) and after the last fourth ISDN injection (day 5). Mean ± SEM, n = 9. * $p<0.05$ with Mann Whitney non parametric test compared to vehicle; # $p<0.05$ with Wilcoxon matched paired test compared to control before injection.

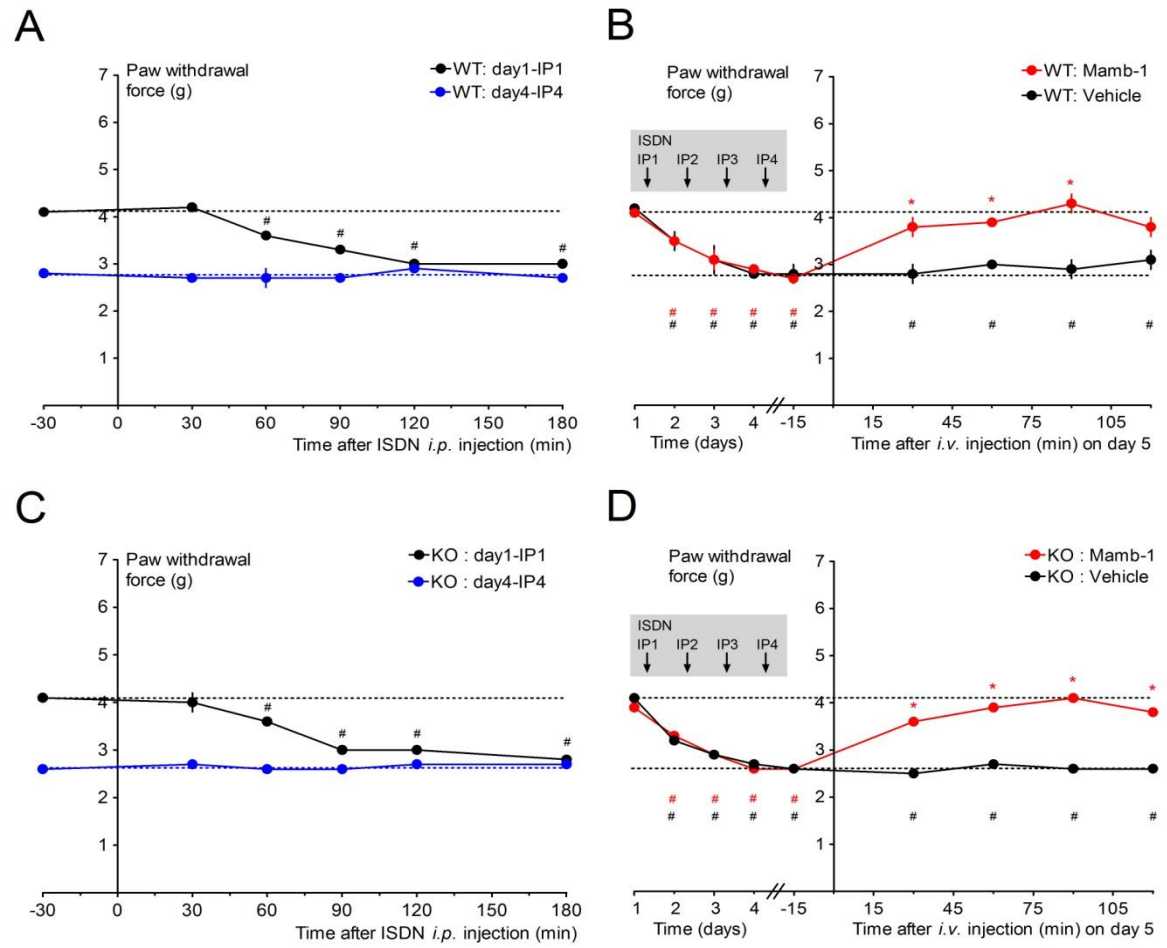

Fig.6: Reversion of ISDN-induced maximal extra-cephalic chronic mechanical allodynia by an intravenous injection of mambalgin-1 in wild-type and ASIC1a knock-out mice.

A, C- Kinetics of the effects of the first ISDN injection on day 1 and of the fourth ISDN injection on day 4 on hindpaw mechanical withdrawal threshold (g) of wild-type (**A**, n=20) and ASIC1a-KO (**C,** n=17) mice. Mean ± SEM, # $p<0.05$ with Wilcoxon matched paired test compared to control value before the ISDN injection, all non significant for day 4 data. **B, D**- Kinetics of the anti-allodynic effect of Mamb-1 (13.6 nmol/kg) and vehicle *i.v.* injected one day after the last ISDN injection (*i.e.*, on day 5) on paw mechanical withdrawal force (g) of wild-type (**B,** n=10) and ASIC1a-KO (**D**, n=8-9) mice. The basal mechanical withdrawal force (g) was measured before each daily ISDN injection (left side of the y axis, which includes the values at -30 min for day 1 and 4 in Fig. 6A and C), showing the chronification process of cutaneous allodynia day after day. Mean ± SEM, n = 8-10. * $p<0.05$ with Mann Whitney non parametric test compared to vehicle; # $p<0.05$ with Wilcoxon matched paired test compared to control value before the first ISDN injection (day 1). Mice used in A and C have been then divided in half to be injected with either vehicle or Mamb-1, as shown in B and D.